Universal phase unwrapping for phase measuring profilometry using geometry analysis

Jianwen Song[a], Yo-Sung Ho[b], Daniel L. Lau[c], and Kai Liu[a,*]

[a]School of Electrical Engineering and Information, Sichuan University, China
[b]School of Electrical Engineering and Computer Science, Gwangju Institute of Science and Technology, Korea
[c]Department of Electrical Engineering, University of Kentucky, USA
[*]Corresponding author: kailiu@scu.edu.cn

ABSTRACT

Traditionally temporal phase unwrapping for phase measuring profilometry needs to employ the phase computed from unit-frequency patterned images; however, it has recently been reported that two phases with co-prime frequencies can be absolutely unwrapped from each other. However, a manually man-made look-up table for two known frequencies has to be used for correctly unwrapping phases. If two co-prime frequencies are changed, the look-up table has to be manually rebuilt. In this paper, a universal phase unwrapping algorithm is proposed to unwrap phase flexibly and automatically. The basis of the proposed algorithm is converting a signal-processing problem into a geometric analysis one. First, we normalize two wrapped phases such that they are of the same needed slope. Second, by using the modular operation, we unify the integer-valued difference of the two normalized phases over each wrapping interval. Third, by analyzing the properties of the uniform difference mathematically, we can automatically build a look-up table to record the corresponding correct orders for all wrapping intervals. Even if the frequencies are changed, the look-up table will be automatically updated for the latest involved frequencies. Finally, with the order information stored in the look-up table, the wrapped phases can be correctly unwrapped. Both simulations and experimental results verify the correctness of the proposed algorithm.

Keywords: Structured Light Illumination, Phase Measuring Profilometry, Temporal Phase Unwrapping, Co-prime Frequencies, Geometric Analysis

1. INTRODUCTION

As one of the well known structured light techniques for 3D reconstruction,[1,2] phase measuring profilometry (PMP)[3] employs high-frequency sinusoid patterns to achieve high accuracy by suppressing error sources, including noise, nonlinearity, etc, in real time.[4,5] In order to remove ambiguities caused by high-frequency light signals, wrapped phase must be correctly unwrapped.[6] Typically, there are two streams of unwrapping, i.e. spatial[7–9] and temporal[10–12] methods. Spatial algorithms suffer from phase discontinuities, phase jumps, error propagating, etc.,[13] and temporal methods are more robust and are of higher speed in unwrapping.[6]

Traditional temporal phase unwrapping needs several groups of phases computed from patterns with different frequencies, including unit frequency.[10] Starting from a unit-frequency phase, wrapped phases with higher frequency can be unwrapped one by one till the highest-frequency phase is unwrapped to be used for final 3D reconstruction. Obviously, in this way, the wrapped high-frequency phase can be unwrapped as correctly as possible. However, the cost is that more additional groups of assisting reference patterns are needed and scanning time is longer.

Recently, Ding et al. have published a series of papers discussing on temporally unwrapping phases by using sinusoid patterns with co-prime frequencies.[14–20] Basically, only one reference phase map with a reference frequency co-primed to the principal frequency is needed to unambiguously unwrap a principal phase map. The process of phase unwrapping needs a man-made look-up table (LUT) which stores the corresponding orders of wraps between the reference patterns and the principal patterns. However, once the principal frequency or/and the reference frequency is/are changed, the LUT has to be rebuilt in a manual manner.

Emerging Digital Micromirror Device Based Systems and Applications X, edited by Michael R. Douglass, Benjamin L. Lee, Proceedings of SPIE Vol. 10546, 105460B
 · doi: 10.1117/12.2289423

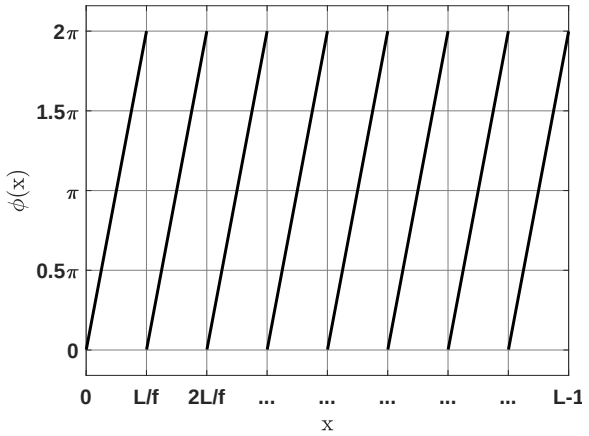

Figure 1. Wrapped ϕ with wraps of f

In this paper, motivated by Ding et al., we propose a universal phase unwrapping algorithm to unwrap phase flexibly and automatically. We build the geometric models for wrapped phases and can easily determine the correct orders for wraps by analyzing the geometric models. A LUT is also used in our solution, but, when frequencies are changed, the LUT can be automatically updated according to the models. Both simulations and experimental results verify the correctness of the proposed algorithm.

2. METHODS

A group of projected PMP patterns with the same spatial frequency, f, are coded as[4]

$$I_n^p\left(x^p, y^p\right) = A^p + B^p \cos\left[2\pi\left(f\frac{y^p}{H} - \frac{n}{N}\right)\right], \tag{1}$$

where I_n^p is the pattern intensities at projector coordinates (x^p, y^p), two constants A^p and B^p hold $A^p \geq B^p$, the integer-valued f is the spatial frequency, the term H is the height of a projector's spatial resolution, and n and N (≥ 3) are the index of a phase shift and the total number of phase shifts, respectively. After one pattern is projected onto a scanned object, a camera immediately captures an image and the patterned image, denoted as I_n^c, is modeled as[4]

$$I_n^c\left(x^c, y^c\right) = A^c\left(x^c, y^c\right) + B^c\left(x^c, y^c\right)\cos\left[\phi\left(x^c, y^c\right) - \frac{2\pi n}{N}\right], \tag{2}$$

where A^c, B^c and ϕ are the direct component, the modulation and the phase, respectively, at camera coordinates (x^c, y^c). Note that I_n^c, A^c, B^c and ϕ are functions of (x^c, y^c), and henceforth we will remove the coordinates notations for the purpose of concise expressions. The direct component A^c, acting as the texture for reconstructed 3D point clouds, is computed by

$$A^c = \frac{1}{N}\sum_{n=0}^{N-1} I_n^c, \tag{3}$$

the modulation component B^c, significantly efficient for removing shadow noise,[4] is computed by

$$B^c = \frac{2}{N}\sqrt{\left[\sum_{n=0}^{N-1} I_n^c \sin\left(\frac{2\pi n}{N}\right)\right]^2 + \left[\sum_{n=0}^{N-1} I_n^c \cos\left(\frac{2\pi n}{N}\right)\right]^2}, \tag{4}$$

and the most important term ϕ, used for 3D reconstruction, is computed by[4]

$$\phi = \tan^{-1}\left[\frac{\sum_{n=0}^{N-1} I_n^c \sin\left(\frac{2\pi n}{N}\right)}{\sum_{n=0}^{N-1} I_n^c \cos\left(\frac{2\pi n}{N}\right)}\right] \tag{5}$$

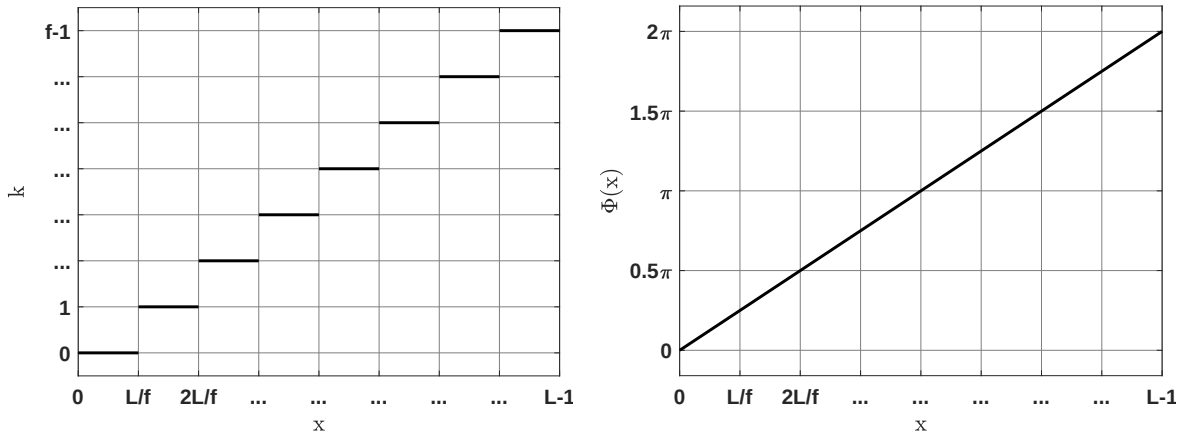

(a) Order of wraps (b) Unwrapped phase

Figure 2. Order of wraps and unwrapped phase

which is mapped to $[0, 2\pi]$ as required in this paper.

In practice, we prefer to use a high frequency, i.e., in Eq. (1), let $f > 1$, to suppress various errors,[5] e.g. noise, nonlinearity, etc. Thus, the phase ϕ, computed by Eq. (5), is exactly wrapped by the factor f, i.e. the wraps of ϕ equals to f, and need to be unwrapped to cancel ambiguities. For the wrapped ϕ shown in Fig. 1, from left to right, its wrap order is $k = 0, 1, \cdots, f-1$, respectively. Once the order k is correctly determined as shown in Fig. 2(a), the absolute phase Φ can be then correctly unwrapped through

$$\Phi = \frac{\phi}{f} + k\frac{2\pi}{f} \tag{6}$$

as shown in Fig. 2(b). In order to temporally unwrap ϕ, we can employ a reference phase, denoted as ϕ^r, generated by another group of PMP patterns with a different frequency f^r. The reference frequency f^r need to be a prime number, including 1, to the wraps of ϕ.[14,15] In Fig. 3, the dash-dot line is ϕ^r with wraps of $f^r = 5$ as example. Note that ϕ and ϕ^r can actually unwrap each other, and we call them as 'phase' and 'reference phase', respectively, just in order to clearly describe the process of automatical unwrapping next. From Fig. 3, for the originally computed ϕ and ϕ^r, it is difficult to visually figure out their relationship. However, from the view of

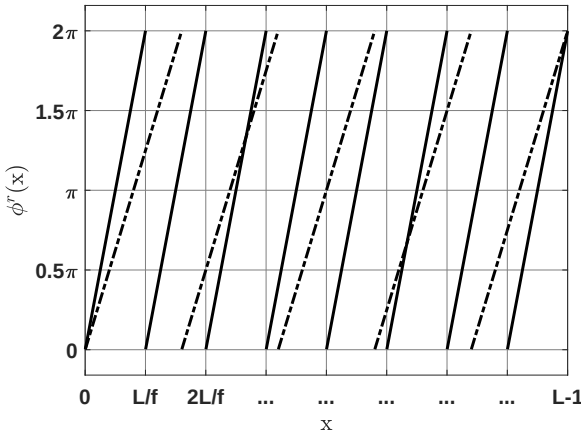

Figure 3. Wrapped ϕ^r with wraps of f^r

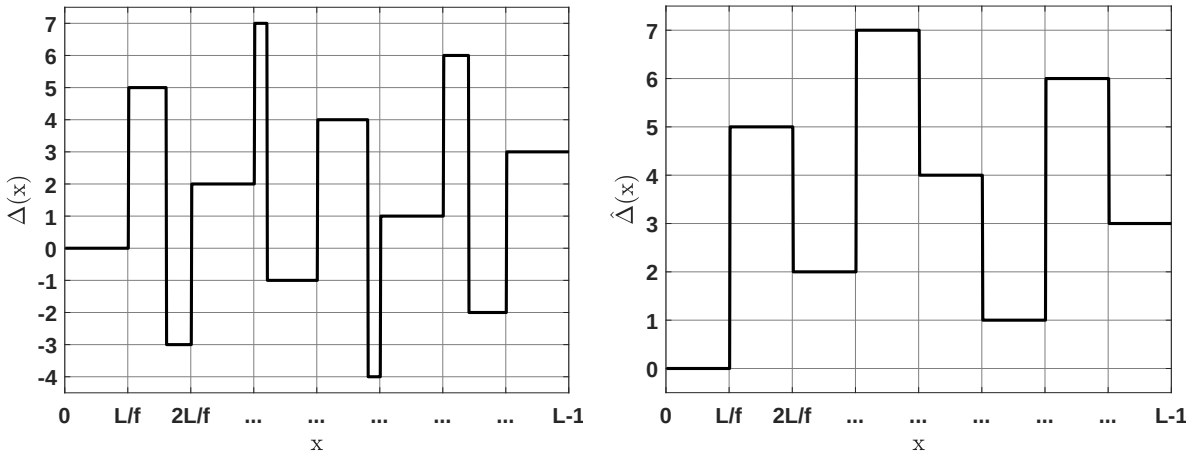

(a) $\Delta(x)$ (b) $\hat{\Delta}(x)$

Figure 4. The difference between $\hat{\phi}$ and $\hat{\phi^r}$

1-D geometry, we know the equation for the curve of ϕ is

$$\begin{aligned} \phi(x) &= 2\pi \frac{f}{L}\left(x\%\frac{L}{f}\right) \\ &= 2\pi\left[\left(f\frac{x}{L}\right)\%1\right] \\ &= 2\pi\left(ft - \lfloor ft \rfloor\right) \end{aligned} \tag{7}$$

and similarly, the equation for the curve of ϕ^r is

$$\phi^r(x) = 2\pi\left(f^r t - \lfloor f^r t \rfloor\right), \tag{8}$$

where integers $x \in [0, L-1]$ and $t = x/L$, the symbol % is defined as the modulo operator, and $\lfloor \cdot \rfloor$ is the floor operation. With rescaling ϕ and ϕ^r by

$$\begin{aligned} \hat{\phi}(x) &= \frac{f^r}{2\pi}\phi(x) \\ &= f^r\left(ft - \lfloor ft \rfloor\right) \end{aligned} \tag{9}$$

and

$$\begin{aligned} \hat{\phi^r}(x) &= \frac{f}{2\pi}\phi^r(x) \\ &= f\left(f^r t - \lfloor f^r t \rfloor\right), \end{aligned} \tag{10}$$

respectively, we then have the difference between $\hat{\phi}$ and $\hat{\phi^r}$ as

$$\begin{aligned} \Delta(x) &= \hat{\phi^r}(x) - \hat{\phi}(x) \\ &= f^r \lfloor ft \rfloor - f \lfloor f^r t \rfloor \end{aligned} \tag{11}$$

which are integers over $[-f^r + 1, f - 1]$ as shown in Fig. 4(a). Within each interval $[kL/f, (k+1)L/f)$ $(k = 0, 1, \cdots, f-1)$, the values of $\Delta(x)$ may look different, but they are equivalent and can be unified by

$$\begin{aligned} \hat{\Delta}(x) &= \Delta(x)\%f \\ &= \left(f^r \lfloor ft \rfloor\right)\%f \\ &= (kf^r)\%f, \end{aligned} \tag{12}$$

Table 1. A LUT automatically built with $f = 8$ and $f^r = 5$.

$(kf^r)\,\%f$	0	1	2	3	4	5	6	7
k	0	5	2	7	4	1	6	3

for $k = 0, 1, \cdots, f-1$, as shown in Fig. 4(b).

For Eq. (12), although we can solve k from $\hat{\Delta}(x)$ by using analytical mathematical methods, e.g. Chinese remainder theorem,[12] an alternative method, i.e. a LUT-based solution, is more efficient in practice. With known f and f^r, a LUT with length of f can be automatically built as

$$\text{LUT}\left[(kf^r)\,\%f\right] = k \tag{13}$$

for $k = 0, 1, \cdots, f-1$. With $\hat{\Delta(x)}$ computed via Eq. (12) and the LUT previously built by using Eq. (13), we can access k by looking up the LUT immediately as

$$k = \text{LUT}\left[\hat{\Delta}(x)\right], \tag{14}$$

and ϕ is finally unwrapped by using Eq. (6). Again, once f or f^r is changed, we can automatically update the LUT by using Eq. (13), and don't need to manually fill out a LUT. Finally, we summarize the procedure of the proposed unwrapping as follows:

1) Given a principal frequency f and a reference frequency f^r, we build a LUT with Eq. (13). For example, if $f = 8$ and $f^r = 5$, the corresponding LUT is shown in Table. 1.
2) For ϕ and ϕ^r computed by using Eq. (5), we rescale them by using Eqs. (9) and (10), respectively.
3) We compute the difference between ϕ and ϕ^r by using Eq. (11) and then unify the difference by using Eq. (12) to obtain $\hat{\Delta}(x)$.
4) We use the values of $\hat{\Delta}(x)$ as indices to access orders, k, of wraps stored in the LUT built in Step 1).
5) With the orders k, we finally unwrap ϕ by using Eq. (6).
6) If f or f^r is not changed, repeat Steps 2)-5) for incoming ϕ and ϕ^r; otherwise Step 1) is needed.

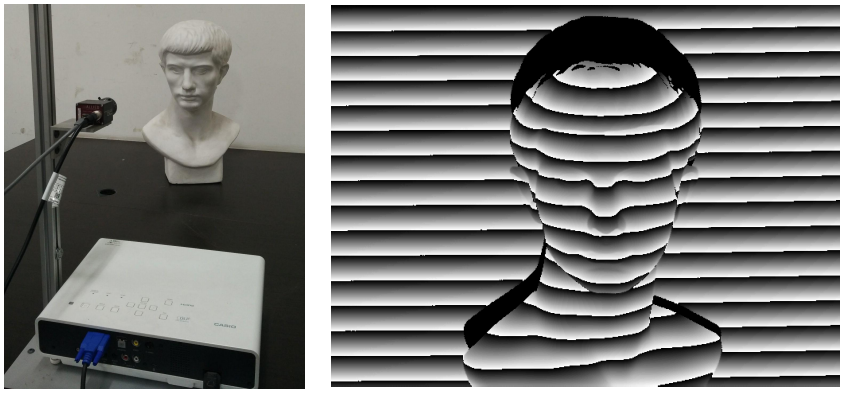

(a) Experimental Setup (b) Wrapped ϕ for $f = 16$

Figure 5. Experimental setup and wrapped phase

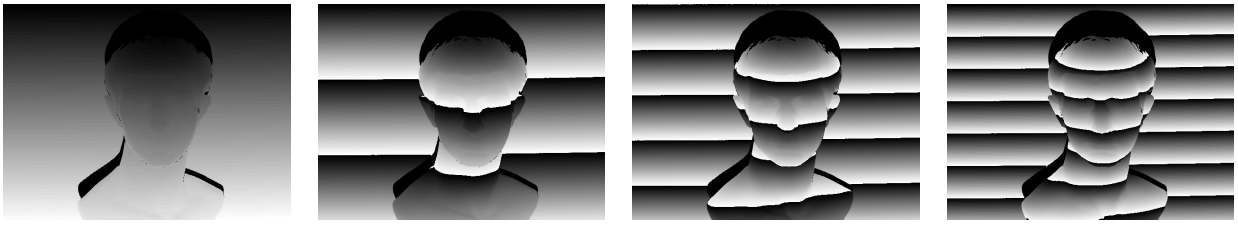

(a) $f^r = 1$ (b) $f^r = 3$ (c) $f^r = 5$ (d) $f^r = 7$

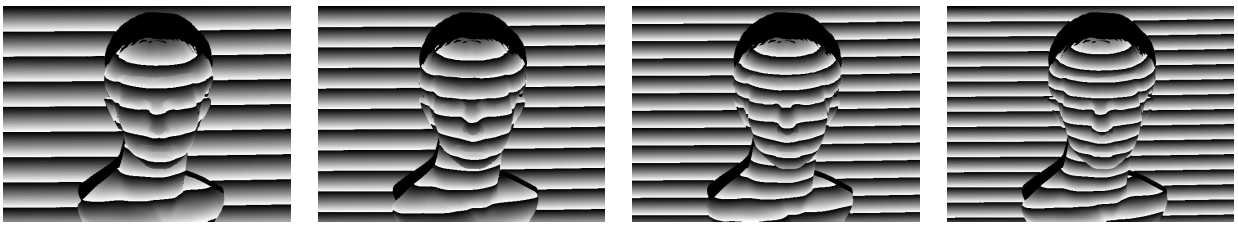

(e) $f^r = 9$ (f) $f^r = 11$ (g) $f^r = 13$ (h) $f^r = 15$

Figure 6. Each reference phase ϕ^r

3. EXPERIMENTAL RESULTS

In this section, we conduct eight groups of experiments to verify the proposed algorithm. As shown in Fig. 5(a), our PMP scanner consists of a Casio XJ-M140 projector working in spatial resolution of 800×600 and an AVT Prosilica GC650 camera working in spatial resolution of 640×480 and grayscale mode; rather than a white flat board, we use a white plaster human statue as the scanned object for a greater challenge; and the controller is an ordinary desktop computer and the software is programmed by using C++ language. The basic settings for generating PMP patterns with Eq. (1) are $A^p = 127.5$, $B^p = 127.5$, and $N = 16$; the principal frequency, i.e. the highest one, finally used for 3D reconstruction is $f = 16$ and the corresponding phase, computed through Eq. (5), is shown in Fig. 5(b); and the reference frequency f^r is one element of $\{2r - 1 | r = 1, 2, \cdots, 8\}$ and the corresponding phase, also computed through Eq. (5), is shown in Figs. 6(a)-6(h), respectively. The shadow noises in the principal phase and each reference phase are removed by using B^c computed through Eq. (4) with a threshold of 10.[4]

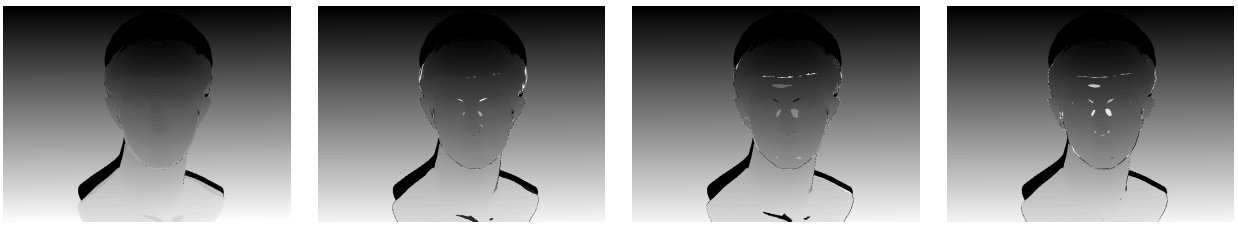

(a) Using $f^r = 1$ (b) Using $f^r = 3$ (c) Using $f^r = 5$ (d) Using $f^r = 7$

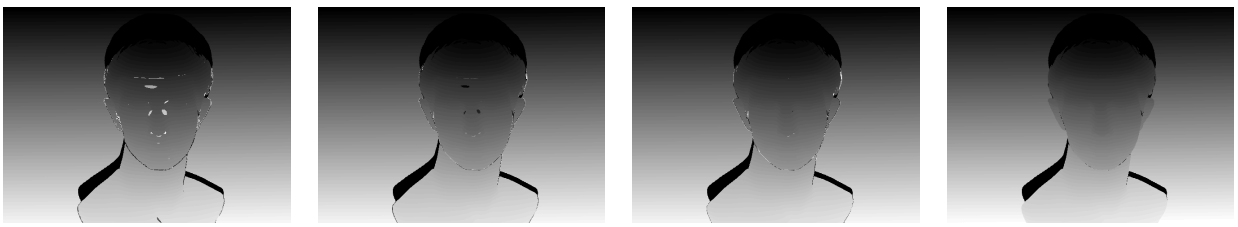

(e) Using $f^r = 9$ (f) Using $f^r = 11$ (g) Using $f^r = 13$ (h) Using $f^r = 15$

Figure 7. Unwrapped phase Φ

(a) Front view (b) Side view

Figure 8. Reconstructed 3D point clouds.

Following the proposed unwrapping procedure summarized in the end of the previous section step by step, we can unwrap the phase ϕ for $f = 16$, shown in Fig. 5(b), with the each reference phase ϕ^r for $f^r = 2r - 1$, respectively, and the each unwrapped phase Φ is shown in Figs. 7(a)-7(h), respectively. In Step 3), for computing the difference $\Delta(x)$, roundoff operation must be used to guarantee that $\Delta(x)$ is integer-valued. Finally, the front view and the side view of the 3D point clouds reconstructed from Φ unwrapped via ϕ^r with $f^r = 15$ are shown in Figs. 8(a) and 8(b), respectively.

Because noise always exists, more or less, there are wrongly-unwrapped Φ. If we employ a phase unwrapped by using traditional multi-frequency PMP as the ground truth, the numbers of wrongly-unwrapped Φ for each f^r are counted and listed in Table. 2 from which we can see that the largest number is for $f^r = 1$ and the least number is for $f^r = 15$, and the number of the wrongly unwrapped is nearly monotonously decreasing with increasing f^r. In our investigation, most of the wrongly unwrapped pixels are actually located at the edges of shadows, and the real wrongly unwrapped are at the face area around the nose of the statue, as obviously shown in Figs. 7(b)-(e). In this paper, although we haven't theoretically analyzed errors, caused by noise, nonlinearity, etc., yet, from Table. 2, it seems that we can simply or temporarily conclude that the optimal reference frequency for a principal frequency f is $f^r = f - 1$. In the future, in our next study, we believe that an optimal reference frequency can be worked out in theory.

4. CONCLUSION

In this paper, we propose a universal phase unwrapping algorithm to unwrap phase flexibly and automatically. We build the geometric models for wrapped phases and can easily determine the orders for wraps with analyzing the geometric models. A LUT is employed in the solution and, when frequencies are changed, a new LUT can be automatically updated without involving manual operations. Both simulations and experimental results verify the correctness of the proposed algorithm. In the future, we will work on a more practicable model with considering the effects of error sources.

Acknowledgments

This work was supported, in part, by the National Natural Science Foundation of China (#61473198) and by the Science and Technology Support Program of Sichuan Province, China (#18ZDYF1655).

Table 2. The number of wrongly unwrapped ϕ for each ϕ^r

f^r	1	3	5	7	9	11	13	15
# of the wrongly unwrapped	3907	2256	2870	1740	1652	1335	891	117
Percentage	1.35%	0.78%	0.99%	0.60%	0.57%	0.46%	0.31%	0.04%

REFERENCES

[1] Salvi, J., Matabosch, C., Fofi, D., and Forest, J., "A review of recent range image registration methods with accuracy evaluation," *Image and Vision Computing* **25**(5), 578–596 (2007).

[2] Geng, J., "Structured-light 3D surface imaging: a tutorial," *Advances in Optics and Photonics* **3**(2), 128–160 (2011).

[3] Srinivasan, V., Liu, H. C., and Halioua, M., "Automated phase-measuring profilometry: a phase mapping approach," *Applied Optics* **24**(2), 185–188 (1985).

[4] Liu, K., Wang, Y., Lau, D. L., Hao, Q., and Hassebrook, L. G., "Dual-frequency pattern scheme for high-speed 3-D shape measurement," *Optics Express* **18**(5), 5229–5244 (2010).

[5] Wang, Y., Liu, K., Hao, Q., Wang, X., Lau, D. L., and Hassebrook, L. G., "Robust active stereo vision using Kullback-Leibler divergence," *IEEE Transactions on Pattern Analysis and Machine Intelligence* **34**(3), 548–563 (2012).

[6] Zuo, C., Huang, L., Zhang, M., Chen, Q., and Asundi, A., "Temporal phase unwrapping algorithms for fringe projection profilometry: A comparative review," *Optics and Lasers in Engineering* **85**, 84–103 (2016).

[7] Goldstein, R. M., Zebker, H. A., and Werner, C. L., "Satellite radar interferometry: Two-dimensional phase unwrapping," *Radio Science* **23**(4), 713–720 (1988).

[8] Zhang, S., Li, X., and Yau, S.-T., "Multilevel quality-guided phase unwrapping algorithm for real-time three-dimensional shape reconstruction," *Applied Optics* **46**(1), 50–57 (2007).

[9] Zhao, M., Huang, L., Zhang, Q., Su, X., Asundi, A., and Kemao, Q., "Quality-guided phase unwrapping technique: comparison of quality maps and guiding strategies," *Applied Optics* **50**(33), 6214–6224 (2011).

[10] Huntley, J. M. and Saldner, H. O., "Error-reduction methods for shape measurement by temporal phase unwrapping," *Journal of the Optical Society of America A* **14**(12), 3188–3196 (1997).

[11] Li, J., Hassebrook, L. G., and Guan, C., "Optimized two-frequency phase-measuring-profilometry light-sensor temporal-noise sensitivity," *Journal of the Optical Society of America A* **20**(1), 106–115 (2003).

[12] Towers, C. E., Towers, D. P., and Jones, J. D., "Time efficient Chinese remainder theorem algorithm for full-field fringe phase analysis in multi-wavelength interferometry," *Optics Express* **12**(6), 1136–1143 (2004).

[13] Wang, Y., Liu, K., Hao, Q., Lau, D. L., and Hassebrook, L. G., "Period coded phase shifting strategy for real-time 3-D structured light illumination," *IEEE Transactions on Image Processing* **20**(11), 3001–3013 (2011).

[14] Ding, Y., Xi, J., Yu, Y., , and Chicharo, J., "Recovering the absolute phase maps of two fringe patterns with selected frequencies," *Optics Letters* **36**(13), 2518–2520 (2011).

[15] Ding, Y., Xi, J., Yu, Y., Cheng, W., Wang, S., and Chicharo, J. F., "Frequency selection in absolute phase maps recovery with two frequency projection fringes," *Optics Express* **20**(12), 13238–13251 (2012).

[16] Ding, Y., Xi, J., Yu, Y., and Deng, F., "Absolute phase recovery of three fringe patterns with selected spatial frequencies," *Optics and Lasers in Engineering* **70**, 18–25 (2015).

[17] Ding, Y., Xi, J., Yu, Y., Deng, F., and Cheng, J., "Multiple spatial-frequency fringes selection for absolute phase recovery," *Surface Topography: Metrology and Properties* **4**(1), 015004 (2016).

[18] Ding, Y., Xi, J., Yu, Y., Deng, F., and Cheng, J., "Recovering the absolute phase maps of three selected spatial-frequency fringes with multi-color channels," *Neurocomputing* **252**, 17–23 (2017).

[19] Ding, Y., Peng, K., Lu, L., Zhong, K., and Zhu, Z., "Simplified fringe order correction for absolute phase maps recovered with multiple-spatial-frequency fringe projections," *Measurement Science and Technology* **28**(2), 025203 (2017).

[20] Ding, Y., Peng, K., Yu, M., Lu, L., and Zhao, K., "Fringe order correction for the absolute phase recovered by two selected spatial frequency fringe projections in fringe projection profilometry," *Review of Scientific Instruments* **88**, 083104 (2017).